© 2022. Published by The Company of Biologists Ltd | Development (2022) 149, dev199841. doi:10.1242/dev.199841

RESEARCH ARTICLE

The Hox gene *Antennapedia* is essential for wing development in insects

Chunyan Fang[1,2], Yaqun Xin[1], Tao Sun[1], Antónia Monteiro[3,4], Zhanfeng Ye[1], Fangyin Dai[1], Cheng Lu[1] and Xiaoling Tong[1,*]

ABSTRACT

A long-standing view in the field of evo-devo is that insect forewings develop without any Hox gene input. The Hox gene *Antennapedia* (*Antp*), despite being expressed in the thoracic segments of insects, has no effect on wing development. This view has been obtained from studies in two main model species: *Drosophila* and *Tribolium*. Here, we show that partial loss of function of *Antp* resulted in reduced and malformed adult wings in *Bombyx*, *Drosophila* and *Tribolium*. *Antp* mediates wing growth in *Bombyx* by directly regulating the ecdysteriod biosynthesis enzyme gene (*shade*) in the wing tissue, which leads to local production of the growth hormone 20-hydroxyecdysone. Additional targets of *Antp* are wing cuticular protein genes *CPG24*, *CPH28* and *CPG9*, which are essential for wing development. We propose, therefore, that insect wing development occurs in an *Antp*-dependent manner.

This article has an associated 'The people behind the papers' interview.

KEY WORDS: Hox, *Antennapedia*, *shade*, 20-Hydroxyecdysone, Cuticular protein gene, Wing development

INTRODUCTION

The Hox genes encode a family of transcriptional regulators that are important in differentiating the bodies of bilaterian animals along their antero-posterior axis (Mallo and Alonso, 2013). Disruptions to individual Hox genes often lead to disruptions of traits that develop in the regions where the Hox gene is expressed (Mallo and Alonso, 2013).

In holometabolous insects, the Hox gene *Antennapedia* (*Antp*) is expressed in all thoracic segments, including the forewing and the hindwing, yet no function has been attributed to this gene regarding wing morphogenesis. In *Drosophila*, wing and haltere primordia can be detected in embryos even in the complete absence of *Antp* function in homozygous mutants of *Antp* (Carroll et al., 1995). In addition, a very low level of Antp protein is detected in the growing wing margin that is not the wing primordium region, indicating that forewing formation does not require Antp (Carroll et al., 1995). Similarly, no obvious phenotypes are observed in adult *Tribolium* elytra (forewing) or hindwing after RNA interference (RNAi) of *Antp*. These data suggest that wing development takes place without any *Antp* input (Tomoyasu et al., 2005). In contrast, the Hox gene *Ultrabithorax* (*Ubx*), which is expressed exclusively in hindwings, functions to differentiate hindwings from forewings. Forewing development in insects was, therefore, thought to occur without any significant Hox gene input (Lewis, 1978; Struhl, 1982; Carroll et al., 1995; Weatherbee et al., 1998; Weatherbee et al., 1999; Roch and Akam, 2000; Deutsch, 2005; Tomoyasu et al., 2005; Pavlopoulos and Akam, 2011; Tomoyasu, 2017; Liu et al., 2020).

Recently, the Antp dose was shown to affect wing morohology in *Drosophila* (Paul et al., 2021). However, the potential downstream genes of Antp in wing disc are unclear. We observed that two loss-of-function mutations in the silkworm *Bombyx mori* *Antp* gene (*BmAntp*), *Nc* and *Wes*, displayed abnormal wings (Nagata et al., 1996; Chen et al., 2013). These mutations have not been examined beyond the embryonic stage due to lethality, but can be maintained in heterozygous lines. The adults of these lines display reduced and malformed wings.

These two *Bombyx Antp* mutants share common features with *Drosophila Antp* mutants that are observable in embryos. The homozygous ($Antp^{-/-}$) embryos die late in embryogenesis but display a homeotic transformation of thoracic legs to antenna-like appendages (Denell et al., 1981; Wakimoto and Kaufman, 1981; Nagata et al., 1996; Chen et al., 2013). The novel wing phenotypes in *Bombyx* heterozygote mutants, however, suggest that *Antp* is affecting wing development, a role not previously documented for this gene, as embryos die long before the stage at which wings start to develop. In the present study, we have used wild-type and heterozygotes of the *Wes* strain ($Antp^{+/-}$), as the study aims to better understand the role of *Antp* in wing development.

RESULTS

BmAntp is involved in the development of wings in *Bombyx*

As defective adult wings were observed in aberrant *Antp Wes* and *Nc* mutants ($Antp^{+/-}$) (Nagata et al., 1996; Chen et al., 2013), we sought to test when in development *Antp* input was required. We analyzed the expression profile of *BmAntp* in the forewing and hindwing of wild-type individuals from the 3rd day of the 5th instar to the adult stage. qRT-PCR revealed that the expression of *BmAntp* was maintained at a low level in the larval stage, and gradually increased and reached a peak on the 6th day of the pupal stage. Forewings expressed higher levels of *Antp* relative to hindwings at most times during the pupal stage (Fig. 1A). We then compared the temporal expression profile of *BmAntp* between mutant *Wes* ($Antp^{+/-}$) and wild-type individuals. *BmAntp* was expressed at a lower level in the mutants compared with wild-type controls from larva to moth stage (Fig. 1B).

[1]State Key Laboratory of Silkworm Genome Biology, Key Laboratory of Sericultural Biology and Genetic Breeding, Ministry of Agriculture and Rural Affairs, Southwest University, Chongqing 400715, China. [2]TCM Regulating Metabolic Diseases Key Laboratory of Sichuan Province, Hospital of Chengdu University of Traditional Chinese Medicine, Chengdu 610072, China. [3]Department of Biological Sciences, National University of Singapore, 14 Sciences Drive 4, 117543 Singapore. [4]Science Division, Yale-NUS College, 10 College Avenue West, 138609 Singapore.

*Author for correspondence (xltong@swu.edu.cn)

F.D., 0000-0002-0215-2177; X.T., 0000-0002-2649-899X

Handling Editor: Cassandra Extavour
Received 30 May 2021; Accepted 9 December 2021

Development (2022) 149, dev199841. doi:10.1242/dev.199841

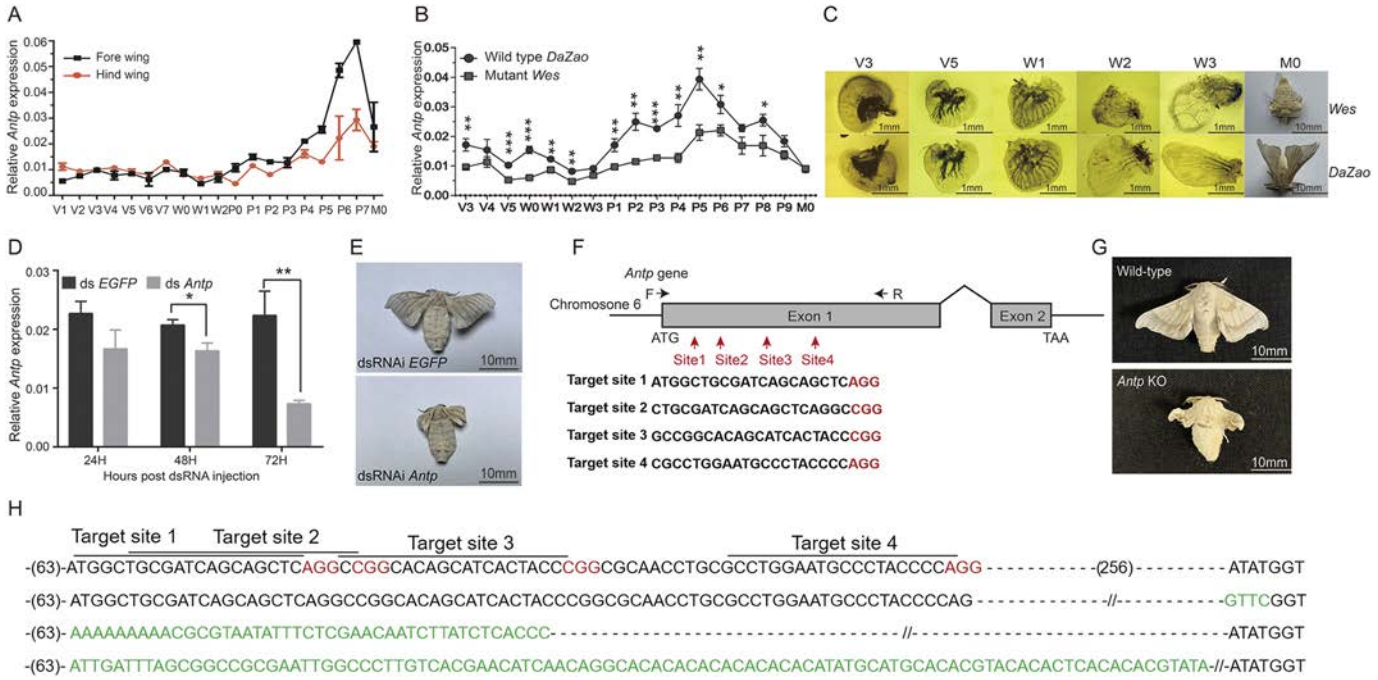

Fig. 1. *Antp* is essential for wing development in *B. mori*. (A) Temporal expression pattern of *Antp* in wild-type (*DaZao*) forewing and hindwing discs by qRT-PCR. (B) Expression profiles of *Antp* in the wing discs of wild-type and mutant (Wes) lines from larvae to adult stages. (C) Phenotype of the wing discs in wild-type *DaZao* and in *Wes* ($Antp^{+/-}$) mutants over different time points. (D) Relative *Antp* expression levels of dsRNA-treated larvae at 24 h, 48 h and 72 h after dsRNA treatments. Animals injected with ds*EGFP* served as controls. (E) Wing phenotype of dsRNA-treated silkworm adults. (F) Genomic structure of *Antp*. The single guide RNA (sgRNA) target sequence is in black font and the protospacer adjacent motif (PAM) sequence is in red font. The red arrows mark the sgRNA targets on the *Antp* gene. F and R indicate the approximate locations of the forward and reverse amplification primers. (G) Representative phenotypes of wild-type (top) and mutated (bottom) insects, with smaller and abnormal wings. (H) Mutated sequences of crispant individuals. The wild-type sequence, shown above the mutant sequences, is in black font and the PAM sequence is in red font. The size of indels is shown on the right of the sequence. Inserted sequenced are in green font. For all graphs, V is the 5th instar larvae; V1-V7 means days 1-7 of the 5th instar larvae; W is the wandering larval stage; W0-W3 indicates days 0-3 of the wandering larval stage; P, the pupal stage; P0-P9 indicates days of 0-9 of the pupal stage; M0, newly emerged adult. All experimental data are mean±s.e.m. (n=3). *P<0.05, **P<0.01, ***P<0.001; two-tailed t-test.

To evaluate the effects of *BmAntp* expression levels on wing morphology during development, we dissected the wing discs of *Wes* ($Antp^{+/-}$) and wild type from the 3rd day of the last larval instar to the wandering stage larva. Wing disc size increased slowly during the larval stage and was not significantly different between *Wes* mutants ($Antp^{+/-}$) and wild-type individuals. Then, during the wandering stage, the wing morphology changed dramatically, leading to wing discs dysplasia in *Wes* mutants ($Antp^{+/-}$), which presented as folded, curled and unexpanded wing discs. Finally, the wing discs of *Wes* mutants ($Antp^{+/-}$) degenerated to tiny and wrinkled adult wings (Fig. 1C, Fig. S1).

To confirm the function of *BmAntp* in wing development, we performed RNAi injections into wild-type larvae of *B. mori*. We synthesized dsRNA targeting *BmAntp* and injected it into larvae on the 1st day of the wandering stage. qRT-PCR showed that *BmAntp* dsRNA efficiently reduced *BmAntp* transcript levels compared with controls injected with *EGFP* dsRNA (Fig. 1D). Nineteen out of 22 (86%) *BmAntp* dsRNA treated individuals had small wings, similar to the *Wes* mutant ($Antp^{+/-}$), whereas control silkworm adults grew their wings normally (Table S2, Fig. 1E).

To further confirm the function of *BmAntp*, we performed CRISPR-Cas9 injections into wild-type embryos of *B. mori*. We generated a genomic disruption of the *BmAntp* gene by targeting its first exon using four specific single-guide RNAs (sgRNAs) and the Cas9/gRNA ribonucleoprotein (RNP) delivery system (Fig. 1F). After injection, 20 eggs hatched and 18 larvae developed to the adult stage. We found that 61% of the moths (11 individuals) displayed malformed adult wings (Fig. 1G), and confirmed that various insertions and deletions were present at the location targeted by the four sgRNAs (Fig. 1H). Abnormal wings were not observed in controls injected with *BmBLOS2* sgRNA, which only led to translucent larval skin. These data indicate that *BmAntp* is a crucial transcription factor that regulates wing development in *B. mori*.

BmAntp affects the synthesis of 20E by regulating the expression of *shade* in wing discs

We next tested whether the production of abnormal wings in *BmAntp* mutants was related to deficits in levels of the molting hormone 20-hydroxyecdysone (20E). We tested this hypothesis because: (1) significant differences in the size of wing discs were observed between *BmAntp* mutants and controls, starting from the onset of the larva-to-pupa transition (Fig. 1C); (2) a pulse of this steroid hormone normally regulates the larva-to-pupa transition; and (3) 20E is a major regulator of wing growth and development (Denell et al., 1981; Wakimoto and Kaufman, 1981).

We first examined the expression level of genes involved in the ecdysteroid biosynthesis pathway in a variety of tissues. We found that *spookier*, *phantom*, *disembodied* and *shadow* were expressed in the prothoracic gland (PG), as expected, as this is the main source of ecdysteroid synthesis in insect larvae (Struhl, 1982). In addition, the *shade* gene, which encodes a P450 monooxygenase that converts ecdysone into the active 20E in targeted peripheral tissues (Mizoguchi et al., 2001), was primarily expressed in the wing discs compared with the PG and hemolymph (Fig. 2A–E).

Development (2022) 149, dev199841. doi:10.1242/dev.199841

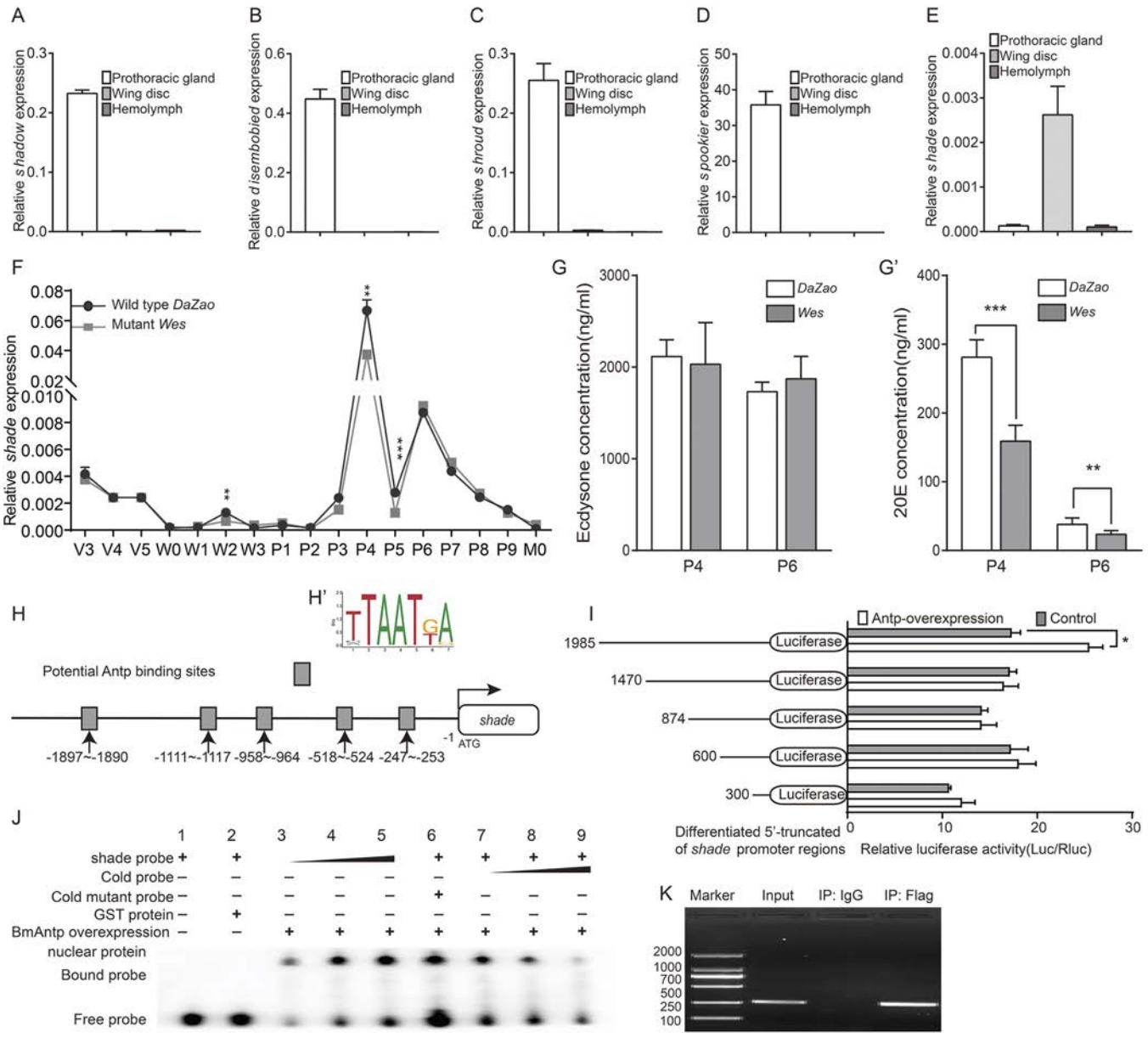

Fig. 2. *Antp* induces 20E synthesis in the wing tissue by directly binding to the *shade* promoter. (A-E) Relative expression of five ecdysteroid enzyme genes in the prothoracic gland, hemolymph and wing disc. (F) mRNA levels of *shade* were detected by qRT-PCR from the 5th instar larval stage to the adult stage. (G,G′) The titers of ecdysone (G) and 20E (G′) in *Bombyx* wing discs of wild-type *DaZao* and *Wes* mutants (*Antp*$^{+/-}$) at P4 and P6. (H) Location of the five potential Antp-binding sites in the *shade* promoter. (H′) Classic Antp-binding motif. (I) The effect of different truncations of the *shade* promoter on luciferase activity when Antp is overexpressed in BmN cells. (J) EMSA confirmed that the recombined Antp proteins bind to the −1897 to −1890 nucleotide region in the *shade* promoter (lane 1). Co-incubating nucleoproteins from *Escherichia coli* strain BL21 (DE3) competent cells overexpressing GST with labeled Antp probes resulted in loss of the binding band (lane 2). Purified recombinant BmAntp protein could bind to the biotinylated probes in a dose-dependent manner (lanes 3-5), and this binding could be competitively suppressed by unlabeled probe (lanes 7-9). The unlabeled probe with mutation in the core-binding motif of BmAntp could not compete for BmAntp binding to biotinylated probes (lane 6). We further validated the direct regulation of *shade* transcription by BmAntp through *in vivo* ChIP-PCR following the BmN cells in which FLAG-tagged BmAntp was overexpressed. (K) ChIP-PCR assay of the direct binding of Antp to the *shade* promoter in BmN cells with Antp-Flag overexpression. Specific primers covering Antp-binding sites of the three *shade* promoters were used. Compared with nonspecific IgG antibody, used as a negative control, the antibody against FLAG can specifically immunoprecipitate the DNA regions, including −1985 to −1470 of the *shade* promoter. All experimental data are mean±s.e.m. (n=3).*P<0.05, **P<0.01, ***P<0.001; two-tailed t-test.

We next explored whether *Wes* mutants (*Antp*$^{+/-}$) expressed *shade* at different levels relative to wild-type wings, and whether this impacted levels of 20E in the wing tissue. The *shade* transcripts were present at higher levels in wild-type than in *Wes* mutant (*Antp*$^{+/-}$) wings, and levels reached a peak on the 4th day of the pupal stage (Fig. 2F). Titers of ecdysone measured from wing discs on that day (P4), were similar between *Wes* mutants (*Antp*$^{+/-}$) and wild-type individuals. Titers of 20E, however, were significantly lower in the *Wes* mutant (*Antp*$^{+/-}$) relative to wild-type wings at P4 and P6 (Fig. 2G,G′).

We next investigated whether the expression levels of *Ecdysone Receptor* (*EcR*) and *ultraspiracle* (*usp*) (Fujiwara and Hojyo, 1997), the receptors that bind 20E to transduce ecdysone signaling to the nucleus, were also different between *Wes* and wild-type individuals.

Development (2022) 149, dev199841. doi:10.1242/dev.199841

This is because 20E signaling is known to upregulate expression of *EcR* and *usp* in the wings of *Drosophila* (D'Avino and Thummel, 2000; Schubiger and Truman, 2000). Significantly lower levels of *usp*, and of the two isoforms of *EcR* (*EcRA* and *EcRB* mRNA) were detected in the mutant compared with wild-type wings on P4 (Fig. S2). These results suggest that Antp is also regulating the expression of these genes, either directly or indirectly. The latter mechanism could involve Antp upregulating *shade*, which increases 20E titers in the wing cells which, in turn, upregulates *EcR* and *usp* transcription in wings.

We next sought to test whether *shade* was a direct target of BmAntp. We examined a 2 kb region of DNA immediately 5′ of the start site of *shade* for potential Antp-binding sites and found a total of five such sites (Fig. 2H,H′). To evaluate the regulatory function of DNA containing one or more of these sites on reporter gene expression, we cloned different sized fragments, containing a different number of Antp-binding sites, upstream of the reporter gene *luciferase*. We transfected this plasmid into *Bm*N cells and also co-transfected *BmAntp* in these cells (Fig. S3). The largest fragment (−1985 to −300), containing all five Antp-binding sites, led to significantly increased luciferase activity compared with the other four fragments (Fig. 2I). These data suggest either that a regulatory region −1985 to −1470 containing a key Antp-binding site or, more likely, that all Antp sites together are required for the transcriptional regulation of *shade*, and that *shade* is likely a direct target of BmAntp.

To determine whether BmAntp protein could directly bind to the *in silico* identified Antp-binding sites of the *shade* promoter, we designed a specific biotinylated probe covering the −1985 to −1470 genomic region of *shade* and conducted electrophoretic mobility shift assay (EMSA) (Fig. 2J). We further validated the direct regulation of BmAntp on *shade* transcription with ChIP-PCR on chromatin from BmN cells expressing recombinant BmAntp protein with a FLAG-tag (Fig. 2K, Fig. S4). This experiment showed that BmAntp binds the tested genomic region in BmN cells, providing extra support for a direct activation of *shade* transcription by BmAntp.

BmAntp directly regulates wing-specific cuticular protein genes

In order to explore potential additional targets of Antp, besides *shade*, that might have contributed to the small wings of adult *Wes* mutants, we investigated the expression of four cuticular protein genes with a known expression profile, which matched that of *Antp,* in both wild type and *Wes* mutants. In particular, expression levels of *CPH28*, *CPG24* and *CPG9* peaked at P5, as did expression of Antp (Fig. 1B) (D'Avino and Thummel, 2000). *CPG11*, by contrast, was expressed primarily during the early 5th instar, and was used as a control gene (Futahashi et al., 2008). Previous work has shown that cuticular proteins are major components of insect wings, and that both EcR-mediated signaling and other transcription factors regulate their very dynamic and specific expression profiles (Riddiford et al., 2000; Petryk et al., 2003; Wang et al., 2010). qRT-PCR analysis showed that the expression levels of *CPH28*, *CPG24*, *CPG9* and *CPG11* in *Wes* ($Antp^{+/-}$) were remarkably lower than those of wild-type P5 wings (Fig. 3A). We explored the direct regulation of these four cuticular proteins by Antp by conducting Luciferase reporter assays in BmN cells with candidate genomic regions (3 kb upstream of each gene) containing putative Antp-binding sites (Fig. 3B). Increasing *BmAntp* levels in these cells significantly upregulated the transcription of *CPH28*, *CPG24* and *CPG9* (Fig. 3C-F), but not *CPG11*. A dual-Luciferase assay with *CPH28* further showed that BmAntp can directly elevate the expression of *CPH28* (Fig. 3G). Moreover, an EMSA and ChIP-PCR assay showed that BmAntp was able to directly bind the *in silico* identified Antp-binding sites in the *CPH28* promoter (Fig. 3H,I, Fig. S5). These results indicate that BmAntp can upregulate the transcription of these three wing cuticular protein genes, and *CPH28* is likely upregulated by a direct interaction of Antp with the promoter of this gene.

To determine whether *CPH28* is essential for wing development, we knocked it down using RNAi. CPH28-siRNA was injected into 18 pupae, and the same quantity of scrambled siRNA sequence was injected in control animals. Levels of *CPH28* decreased significantly in the wing discs 48 h after *CPH28*-siRNA injections relative to control injections (Fig. 3J). The ratio of malformed wings reached 80% after eclosion (Fig. 3K, Table S3). In contrast, all moths in the control group had normal wings (Fig. 3K). These results indicate that *CPH28* is required for the generation of normal wings in silkworms.

Antp function in wing development is conserved in *Drosophila* and *Tribolium*

To evaluate whether the function of *Antp* in wing development is conserved across other insect orders, we examined the wings of adult flies and beetles after *Antp* downregulation. In *Drosophila*, we drove expression of *Antp* RNAi hairpins in larval and pupal wing discs under the control of the *nubbin-gal4* (*nub-gal4*) driver. All individuals in which *Antp* was knocked down had rudimentary wings that were reduced in size compared with controls (Fig. 4A-D, Fig. S6A-D). In *Tribolium*, we injected *Antp*/*ptl* dsRNA during the last larval stage, immediately before the onset of rapid wing growth (Tomoyasu et al., 2005). These injections led to lower mRNA levels of *Antp*/*ptl* (Fig. S7A) and to wrinkled and shortened forewings (elytra) and hindwings (Fig. 4E-J, Figs S6E-H, S7B,C). Additionally, the uniform mesonotum phenotype observed in the *Antp*/*ptl* RNAi adults was consistent with that reported by Tomoyasu and colleagues (Figs 4K,L, Fig. S7D,E) (Tomoyasu et al., 2005). These observations indicate that *Antp* plays a crucial role in the development of wings in *Drosophila* and *Tribolium*. Taken together, these results demonstrate that *Antp* participates in insect wing development in a conserved manner.

DISCUSSION

Hox gene *Antp* is indispensable for wing development

Limited experiments in previous *Drosophila* studies, focusing on embryonic and larval stages, likely prevented the identification of a role for Antp in later stages of wing development. Fly embryos homozygous for $Antp^{W10}$, a mutation in the *Antp* sequence, led to normal wing primordia, whereas ectopic expression of *Antp* in third instar larval wing discs had no effect on larval wing disc morphology (Carroll et al., 1995). In the present study, the *nub-Gal4* driver was used to drive *UAS-*$Antp^{RNAi}$ expression in fly wing discs. We chose this driver as its expression was first detected in late 2nd instar wing discs and persisted through late pupal wings (Cifuentes and García-Bellido, 1997). This led to a prolonged silencing of *Antp* expression and to malformed adult wings in *Drosophila*. Recently, an improved immunofluorescence assay in *Drosophila* wing discs using a more recent 8C11 anti-Antp antibody showed that Antp is dynamically expressed in the wing pouch from L1 to L3 larval stages (Paul et al., 2021). In addition, knockdown of *Antp* expression in the whole pouch of wing discs caused reduced wing size and weak margin defects, indicating that *Antp* was required for adult wing blade formation (Paul et al., 2021).

Development (2022) 149, dev199841. doi:10.1242/dev.199841

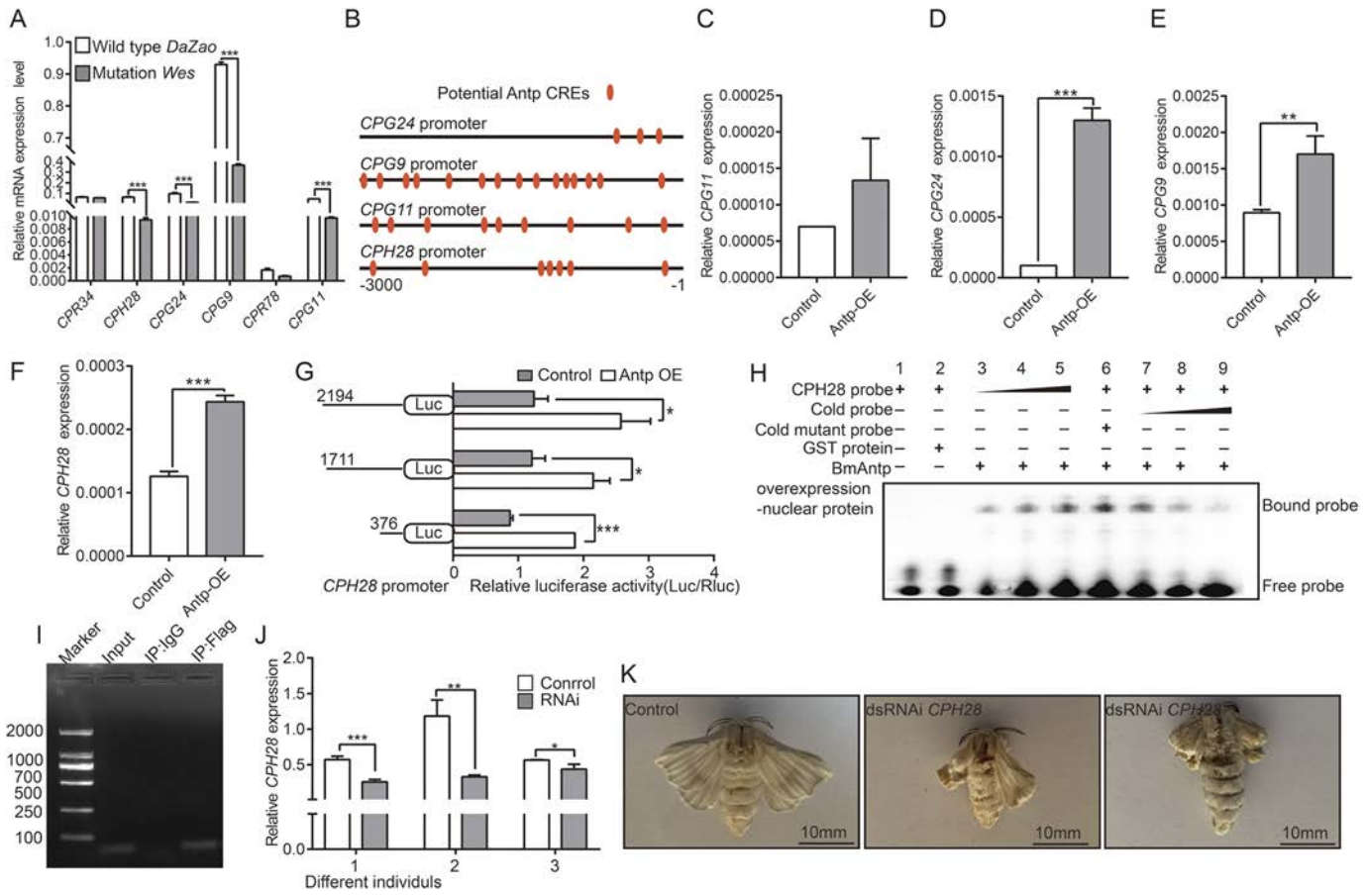

Fig. 3. *Antp* regulates the expression of cuticular protein genes essential for wing development. (A) mRNA levels of cuticular protein genes in wing discs of *DaZao* and *Wes* (*Antp*$^{+/-}$) at P5. (B) Schematic of the potential Antp CREs in the promoters of cuticular protein genes. (C-F) Relative cuticular protein genes expression detected in Antp overexpression BmN cells. (G) Antp increased luciferase activity driven by different truncations of the CPH28 promoter. (H) Electrophoretic mobility shift assay (EMSA) of the binding nuclear proteins extracted from Antp-overexpressing *Escherichia coli* strain BL21 (DE3) competent cells with the Antp-binding motif. Co-incubating nucleoproteins from *E. coli* strain BL21 (DE3) competent cells overexpressing glutathione S-transferase (GST) with labeled Antp probes results in loss of the binding band. The binding signal between recombinant GST-BmAntp protein and Antp-binding motif probe was gradually enhanced with increased probe levels (lanes 3-5). (I) ChIP-PCR assay shows that Antp binds directly to Antp-binding motifs present in the *CPH28* promoter in BmN cells. A Flag tag was fused to BmAntp and an anti-Flag tag antibody was used in the ChIP assay. The cells were transfected with recombinant plasmid Flag-BmAntp, and then the cells were collected for ChIP assay 48 h post-transfection. The results showed that the anti-Flag antibodies, but not IgG (a negative control), precipitated DNA containing the Antp-binding motifs in the cells transfected with the Flag-BmAntp-expressing plasmid. (J) qPCR analyses of *CPH28* expression in wing discs of different individuals 48 h after knock down of *CPH28* and of a control sequence (containing the scrambled siRNA sequence). (K) Comparisons of adult wing morphology after dsRNA injections. All experimental data are mean±s.e.m. (n=3). *P<0.05, **P<0.01, ***P<0.001; two-tailed t-test.

Thus, we speculate that there is little requirement for Antp function during the embryo stage, but Antp is important for wing development in the later larval and pupal stages.

Our RNAi experiment in *Tribolium castaneum* also identified strong wing defects that were not previously identified in a similar RNAi experiment (Tomoyasu et al., 2005). This previous study only reported variation of mesonotum morphology (Tomoyasu et al., 2005), which was also found in our experiments. We performed the *Antp* RNAi experiment twice (>250 individuals) and obtained consistent defective wing morphologies that were not observed in control animals injected with dsRNA against *EGFP*. We speculate that the different outcomes of the two experiments might be due to the different ds*Antp* fragments used. We used two fragments covering a larger region of the *Antp* gene (922 bp) compared with the 535 bp fragment used by Tomoyasu et al. (2005). Based on the present results, we propose that *Antp* is necessary for wing development in *Bombyx*, *Drosophila* and *Tribolium*.

Recently, *Antp* input was found to be required for the development of two novel traits in the wings of the nymphalid butterfly *Bicyclus anynana*: silver scales and eyespot patterns, in both forewings and hindwings, but only minor wing growth deformities were reported (Matsuoka and Monteiro, 2021). It is possible that the role of *Antp* has shifted from a general wing growth role to a more specialized role in color pattern formation. This might be the case in this species and in other nymphalids where *Antp* expression has been visualized in the eyespots (Cifuentes and García-Bellido, 1997; Hombría, 2011). Alternatively, the mosaic disruptions obtained with this CRISPR-Cas9 experiment were insufficient to uncover a more general role of *Antp* in wing growth and development. Most interestingly, the effect of Antp on *shade* expression should be investigated in connection with 20E-mediated eyespot size plasticity in this species (Cifuentes and García-Bellido, 1997; Hombría, 2011).

Antp controls the biosynthesis of 20E in wing discs by *shade*

We showed that Antp directly binds to the promoters of *shade*, a gene encoding the last step in the production of the active ecdysteroid 20E, and that 20E was produced inside wing tissues from the precursor ecdysone produced in the prothoracic gland (Petryk et al., 2003;

Development (2022) 149, dev199841. doi:10.1242/dev.199841

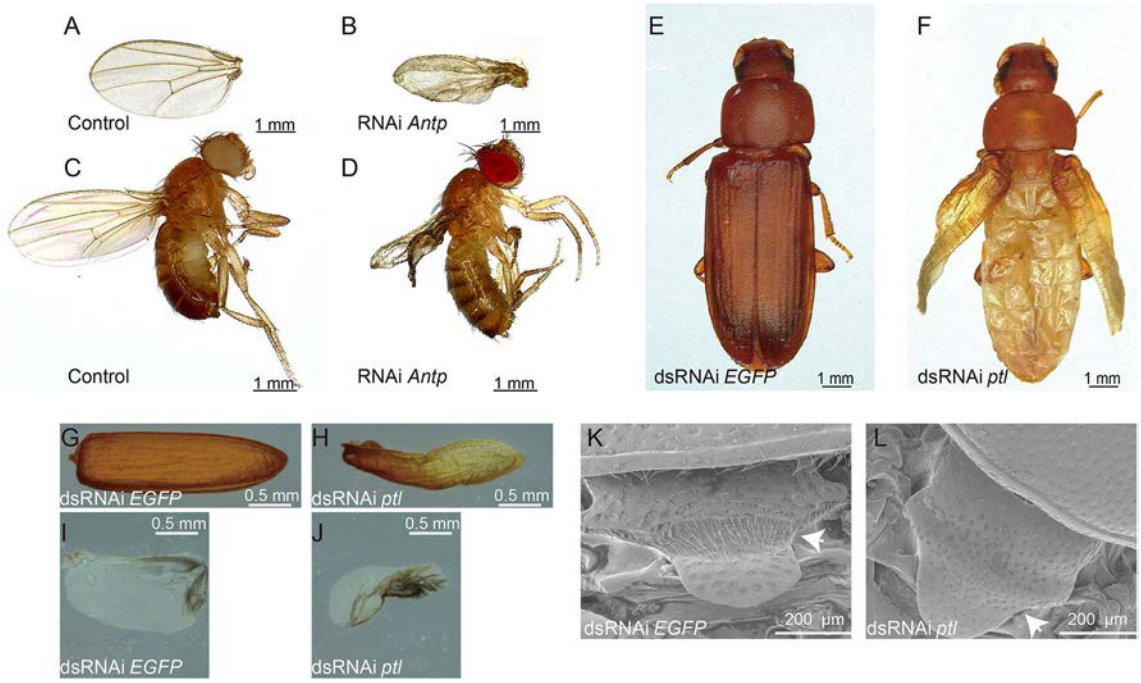

Fig. 4. *Antp* is essential for wing development in *Drosophila* and *Tribolium*. (A,B) Adult *Drosophila* wings from control (A) and *Antp* RNAi-treated (B) individuals. (C,D) Adult *Drosophila* of control (C) and *Antp* RNAi-treated (D) individuals. (E,F) *ptl* RNAi leads to reduction of elytra and hindwings in *Tribolium* adults. (E) ds-*EGFP*. (F) ds-*ptl*. (G,I) The elytron (G) and hindwing (I) from a ds-*EGFP*-treated individual. (H,J) The elytron (H) and hindwing (J) from a ds-*ptl*-treated individual. (K,L) *ptl* RNAi leads to a uniform mesonotum (white arrows in K and L). (K) ds-*EGFP*. (L) ds-*ptl*.

Rewitz et al., 2006). The biosynthesis of 20E, the main hormonal regulator of molting and methamorphosis in insects (Wakimoto and Kaufman, 1981; Shahin et al., 2018), is mediated by the Halloween genes, such as *spookier*, *shroud*, *disembodied*, *shadow* and *shade* (Gilbert and Warren, 2005). *shade* is known to convert ecdysone into 20E in peripheral organs such as the fat body, midgut and Malpighian tubules (Petryk et al., 2003; Rewitz et al., 2006). As expected, the mRNA encoding *shade* was present at an extremely low levels in the prothoracic gland and also in the hemolymph, but at a higher levels in wing discs. Given that the mRNA expression of *shade* in wing discs of *Wes* ($Antp^{+/-}$) mutants was significantly lower than that in normal wing discs, this explains the observed lower levels of 20E, but not of ecdysone, in the wing tissue of these mutants, and associated wing disc growth disruptions.

Antp regulates the expression of wing cuticular protein genes

Cuticular proteins are major components of insect wings and previous studies had already implicated the regulation of these proteins by other Hox genes (Futahashi et al., 2008; Shahin et al., 2018). A total of 52 cuticular protein genes were detected in silkworm wing discs by expressed sequence tags (Futahashi et al., 2008). One of those detected proteins, BmWCP4, has previously been shown to be regulated by the co-binding of the Hox gene *BmAbd-A* with *BmPOUM2*, in the promoter region of the gene (Ou et al., 2014). In the present study, we focused on investigating wing cuticular protein genes whose expression patterns were largely congruent with that of *Antp* (Shahin et al., 2018). We showed that they were remarkably downregulated in mutant ($Antp^{+/-}$) individuals, and that disruptions to one of these proteins impaired wing development. It is possible that many more additional *Antp* targets remain to be described.

Previous studies have assumed that the forewing is a Hox-free wing (Struhl, 1982; Weatherbee et al., 1998; Tomoyasu et al., 2005). Our data indicate that *Antp* is crucial for wing development in insects (Fig. 5). It does this by directly enhancing transcription of the steroidogenic enzyme gene *shade* in wings and, thus, controlling the synthesis of an essential growth hormone, 20E, directly in the wing tissue.

MATERIALS AND METHODS

Animal strains

The mutant strains *Wes* were homeotic mutations caused by a single gene *BmAntp* mutation (Chen et al., 2013). The homozygous ($Antp^{-/-}$) embryos

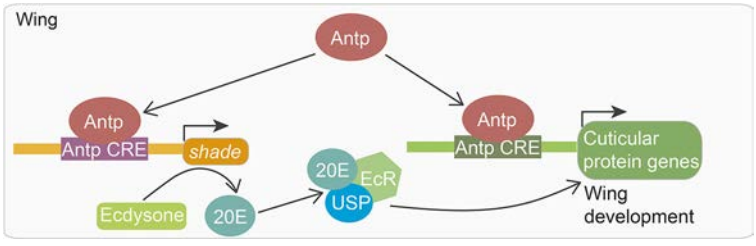

Fig. 5. Proposed model on how *Antp* regulates wing development in *B. mori*. The Hox gene *Antp* plays an essential role in wing development. It does this by directly enhancing transcription of the steroidogenic enzyme gene *shade* in wings and, thus, controlling the synthesis of an essential growth hormone, 20E, directly in the wing tissue. Antp also directly regulates the expression of crucial cuticular protein genes in both forewings and hindwings.

Development (2022) 149, dev199841. doi:10.1242/dev.199841

are all lethal and display a transformation of thoracic legs to antenna-like appendages. Whereas the $Antp^{+/-}$ heterozygote can be completely viable, we observed that all of the heterozygote adults exhibit reduced and malformed wings. We therefore used the heterozygote *Wes* mutation to explore the role of *Antp* on wing development in this study. The wild-type strain *DaZao* and mutant strain *Wes* ($Antp^{+/-}$) were obtained from the Silkworm Gene Bank of Southwest University, China. Silkworms were reared on mulberry leaves at 25°C in ∼75% relative humidity with a 12:12 h (light:dark) photoperiod during their entire life.

The following fly stocks were used in this study: the wild-type *yw* and *nub-gal4* enhancer trap lines (BCF391#) were obtained from Core Facility of Drosophila Resource and Technology. The *UAS-Antp*^{RNAi} (THU2760) was supplied by the Tisng Hua Fly Center. The wild-type *yw* were used as control flies. All individuals were incubated at 25°C.

The *Tribolium castaneum GA-1* strain was used in this study. Insects were reared in whole-wheat flour containing 5% brewer's yeast at 30°C under standard conditions.

Bombyx cell lines

The *Bombyx mori* ovary-derived cell line BmN was cultured at 27°C in TC-100 medium (United States Biological) supplemented with 10% fetal bovine serum (Gibco) and 2% penicillin/streptomycin (Gibco).

RNA extraction and qRT-PCR

Total RNA samples were isolated from wing discs, prothoracic glands, hemolymph, BmN cells and the whole beetles at different time points or under different conditions, using the MicroElute Total RNA kit (Omega) in accordance with manufacturer instructions. The cDNA was synthesized with 1 µg total RNA using the PrimeScript RT Reagent Kit with gDNA Eraser (TaKaRa). qRT-PCR was performed using a qTOWER^{3}G system (Analytikjena) and a qPCR SYBR Green Master Mix (Yeasen). The eukaryotic translation initiation factor 4A (BmMDB probe ID sw22934) was used as an internal reference in *Bombyx*, and ribosomal protein S3 (*rps3*) was used as an internal reference in *Tribolium castaneum*. All experiments were independently performed with three biological replicates and the results were calculated using the 2−ΔΔCT method. Primers are listed in Table S1.

RNAi experiment in *Bombyx* and *Tribolium*

The double-strand RNA (dsRNA) of *Antp*, *CPH28*, *ptl*1, *ptl*2 and *EGFP* were synthesized using the RiboMAX Large Scale RNA Production System T7 kit (Promega). Approximately 100 µg of synthesized ds*Antp* was injected into the second chest spiracle at the first day of *Bombyx* larval wandering stage. We injected 0.4-0.5 µg of ds*ptl* at the ratio of 1:1 mix *ptl*1and *ptl*2 final instar larvae of *Tribolium castaneum*. To knock down *CPH28* expression in the silkworm pupal stage, the siRNA sites 5′-GCAGCAAUUGUUCGCACAATT-3′ and 5′-GGAAGCUUUACAUUC-GGUUTT-3′ (GenePharma) for CPH28 were designed. Ten µl of siRNA (1 µg/µl) was injected from the breathing-valve into the wing disc on the 4th day of the pupal stage. In addition, after injection, all insects were reared in a suitable living environment until analysis.

Downregulation of *Antp* in *Drosophila* wings

We used the Gal4/UAS system to knockdown *Antp* gene expression in *Drosophila* wings. We crossed the *UAS-Antp*^{RNAi} males with *nub-gal4* virgin females and then incubated them at 25°C on a yeast/saccharose medium. The wing phenotypes of F1 adults were observed.

CRISPR/Cas9-mediated *Antp* knockout in *Bombyx*

The sgRNAs for knocking out *Antp* was designed by http://crispr.dbcls.jp/ and synthesized using the RiboMAXTM Large Scale RNA Production System T7 kit (Promega). Cas9 protein was purchased from Invitrogen (Thermo). The four sgRNAs and the Cas9 protein were mixed at a dose of 500 ng/µl. The mixture was incubated for 15 min at 37°C to produce a ribonuclearprotein complex (RNP) and micro-injected into the silkworm embryos within 2 h post oviposition. The injected embryos were incubated at 25°C and >90% relative humidity until they hatched. Genomic DNA of adult wings was extracted using the DNAzol (Takara) according to the manufacturer protocol. The target region was amplified using site-specific primers (Table S1). PCR products were checked by PAGE gel and sequencing approach. Related promoters are listed in Table S1. These sgRNAs synthesized *in vitro* were mixed with Cas9 protein and micro-injected into preblastoderm embryos of the *DaZao* strain.

ELISA

ELISA was used to calibrate the ecdysteroid titer in wing disc of wild type and Antp mutants. Silkworm wing discs were collected from ∼50 pupae, and the pooled sample homogenized in methanol. The homogenate was centrifuged and we evaporated the supernatant at 55°C. The solid matter remaining was redissolved in 1 ml EIA buffer (Cayman Chemical) for 20E measurement and 1 ml sample diluents (BIOHJ) for ecdysone measurement, respectively. Ecdysteroid titers were assayed by an ELISA kit, according to manufacturer instructions (Cayman Chemical or BIOHJ). Absorbance was measured at 414 nm for Cayman kit or 450 nm for BIOHJ kit on a BioTek H1 microplate reader.

20E application

For 20E treatment in *Bombyx* and BmN cells, 20E (Adooq) was dissolved in DMSO and then diluted to the experimental concentrations with deionized distilled water. The final concentration of DMSO was 0.1% (v/v) in water. A total of 4 µg 20E was injected into larvae at the mesothoracic region on the 1st day of the larval wandering stage. An equal volume of DMSO at a final concentration of 0.1% (v/v) was used as the control. After 24 h, the wing discs were dissected in TRK lysis buffer (Omega). 20E (5 µm) was applied to BmN cells for 24 h and then collected. An equal volume of DMSO was used as the control.

Dual luciferase assay

The different lengths of *shade*, *CPH28* and *Antp* promoters were subcloned into the pGL3-basic vector (Promega). The ORF of red fluorescent protein gene (*RFP*)-fused *Antp* was inserted into a pIZ/V5-His vector (Invitrogen) driven by the OpIE2 promoter. Different truncated promoters of pGL3-basic vector were co-transfected with pIZ/V5-His-Antp or treated with 20E at a concentration of 5 µM. After ∼24 or 48 h transient transfection, dual-luciferase activities were measured using the Dual-Glo Luciferase Assay Kit (Promega). A pRL-TK vector containing the Renilla luciferase gene was used as an internal control.

EMSA

The full-length recombinant Antp nuclear proteins were extracted from *E. coli* strain BL21 (DE3) competent cells (TransGen). The potential Antp-binding sites of the *shade* and *CPH28* promoters were predicted by the GENOMATIX system (http://www.genomatix.de/solutions/index.html) and JASPAR CORE (http://jaspar.genereg.net/). The DNA oligonucleotides containing Antp-binding sites were labeled with biotin at the 5′-end and annealed to generate probes. EMSA experiments were conducted according to manufacturer instructions for the EMSA/Gel-Shift Kit (Beyotime). The binding reactions were performed with 4 µg recombinant Antp protein and different amounts of biotin-labeled probes (10 pmol, 20 pmol and 40 pmol) for 30 min at room temperature. For competition assays, 40 pmol unlabeled competitor probes were added to the reaction mixture. These samples were electrophoresed on 5% polyacrylamide gels in 0.5×TBE at room temperature. The total probes are listed in Table S1.

ChIP assay

To further detect the effects of Antp on the activity of the *shade* and *CPH28* promoters, the ChIP assay was performed following kit instructions (GST). BmN cells were transfected with a *Flag-Antp* expression vector and harvested at 48 h. These cells were fixed with 37% formaldehyde, and then DNA-containing proteins were sonicated to obtain 200-1000 bp DNA fragments. The immunoprecipitation reactions were enriched with 1 µg antibody against Flag or IgG. The precipitated DNA and input were used for PCR analysis. The primers used for amplifying the sequences containing potential Antp-binding sites are listed in Table S1.

Statistical analysis

Statistical analyses were performed using GraphPad Prism 7 (GraphPad Software). The data are mean±s.e.m. The differences between two sets of data were analyzed with a two-tailed Student's *t*-test. A value of $P<0.05$ was considered statistically significant: $*P<0.05$, $**P<0.01$ and $***P<0.001$.

Acknowledgements

We thank members of the Tong lab for initial discussions on the paper and three anonymous reviewers for comments that improved the article. We are grateful to the Core Facility of Drosophila Resource and Technology and to the Tisng Hua Fly Center for fly stocks.

Competing interests

The authors declare no competing or financial interests.

Author contributions

Conceptualization: X.T., C.F.; Methodology: C.F., Y.X., T.S., X.T.; Validation: C.F., X.T.; Formal analysis: C.F., X.T.; Investigation: C.F., X.T.; Data curation: C.F., Y.X., T.S., A.M., X.T.; Writing - original draft: C.F.; Writing - review & editing: X.T., A.M., Z.Y., F.D., C.L.; Supervision: X.T., F.D., C.L.; Project administration: X.T.; Funding acquisition: X.T., A.M.

Funding

This work was supported by the National Natural Science Foundation of China (U20A2058 and 31830094). A.M. acknowledges support from the National Research Foundation Singapore Investigatorship award (NRF-NRFI05-2019-0006).

Peer review history

The peer review history is available online at https://journals.biologists.com/dev/article-lookup/doi/10.1242/dev.199841.

References

Carroll, S. B., Weatherbee, S. D. and Langeland, J. A. (1995). Homeotic genes and the regulation and evolution of insect wing number. *Nature* **375**, 58-61. doi:10.1038/375058a0

Chen, P., Tong, X. L., Li, D. D., Fu, M. Y., He, S. Z., Hu, H., Xiang, Z. H., Lu, C. and Dai, F. Y. (2013). Antennapedia is involved in the development of thoracic legs and segmentation in the silkworm, Bombyx mori. *Heredity* **111**, 182-188. doi:10.1038/hdy.2013.36

Cifuentes, F. J. and García-Bellido, A. (1997). Proximo-distal specification in the wing disc of Drosophila by the nubbin gene. *PNAS* **94**, 11405-11410. doi:10.1073/pnas.94.21.11405

D'Avino, P. P. and Thummel, C. S. (2000). The ecdysone regulatory pathway controls wing morphogenesis and integrin expression during Drosophila metamorphosis. *Dev. Biol.* **220**, 211-224. doi:10.1006/dbio.2000.9650

Denell, R. E., Hummels, K. R., Wakimoto, B. T. and Kaufman, T. C. (1981). Developmental studies of lethality associated with the Antennapedia gene complex in Drosophila melanogaster. *Dev. Biol.* **81**, 43-50. doi:10.1016/0012-1606(81)90346-8

Deutsch, J. (2005). Hox and wings. *BioEssays* **27**, 673-675. doi:10.1002/bies.20260

Fujiwara, H. and Hojyo, T. (1997). Developmental profiles of wing imaginal discs of flügellos(fl), a wingless mutant of the silkworm, Bombyx mori. *Dev. Genes Evol.* **207**, 12-18. doi:10.1007/s004270050087

Futahashi, R., Okamoto, S., Kawasaki, H., Zhong, Y.-S., Iwanaga, M., Mita, K. and Fujiwara, H. (2008). Genome-wide identification of cuticular protein genes in the silkworm, Bombyx mori. *Insect Biochem. Mol. Biol.* **38**, 1138-1146. doi:10.1016/j.ibmb.2008.05.007

Gilbert, L. I. and Warren, J. T. (2005). A molecular genetic approach to the biosynthesis of the insect steroid molting hormone. *Vitam. Horm.* **73**, 31-57. doi:10.1016/S0083-6729(05)73002-8

Hombría, J. C.-G. (2011). Butterfly eyespot serial homology: enter the Hox genes. *BMC Bio.* **9**, 26-26. doi:10.1186/1741-7007-9-26

Lewis, E. B. (1978). A gene complex controlling segmentation in Drosophila. *Nature* **276**, 565-570. doi:10.1038/276565a0

Liu, F., Li, X., Zhao, M., Guo, M., Han, K., Dong, X., Zhao, J., Cai, W. and Zhang, Q. (2020). Ultrabithorax is a key regulator for the dimorphism of wings, a main cause for the outbreak of planthoppers in rice. *National Science Review* **7**, 1181-1189. doi:10.1093/nsr/nwaa061

Mallo, M. and Alonso, C. R. (2013). The regulation of Hox gene expression during animal development. *Development* **140**, 3951-3963. doi:10.1242/dev.068346

Matsuoka, Y. and Monteiro, A. (2021). Hox genes are essential for the development of eyespots in Bicyclus anynana butterflies. *Genetics* **217**, 1-9. doi:10.1093/genetics/iyaa005

Mizoguchi, A., Ohashi, Y., Hosoda, K., Ishibashi, J. and Kataoka, H. (2001). Developmental profile of the changes in the prothoracicotropic hormone titer in hemolymph of the silkworm Bombyx mori: correlation with ecdysteroid secretion. *Insect Biochem. Mol. Biol.* **31**, 349-358. doi:10.1016/S0965-1748(00)00127-2

Nagata, T., Suzuki, Y., Ueno, K., Kokubo, H., Xu, X., Hui, C., Hara, W. and Fukuta, M. (1996). Developmental expression of the Bombyx Antennapedia homologue and homeotic changes in the Nc mutant. *Genes Cells* **1**, 555-568. doi:10.1046/j.1365-2443.1996.d01-260.x

Ou, J., Deng, H.-M., Zheng, S.-C., Huang, L.-H., Feng, Q.-L. and Liu, L. (2014). Transcriptomic analysis of developmental features of Bombyx mori wing disc during metamorphosis. *BMC Genomics* **15**, 820. doi:10.1186/1471-2164-15-820

Paul, R., Giraud, G., Domsch, K., Duffraisse, M., Marmigère, F., Khan, S., Vanderperre, S., Lohmann, I., Stoks, R., Shashidhara, L. S. et al. (2021). Hox dosage contributes to flight appendage morphology in Drosophila. *Nat. Commun.* **12**, 2892. doi:10.1038/s41467-021-23293-8

Pavlopoulos, A. and Akam, M. (2011). Hox gene Ultrabithorax regulates distinct sets of target genes at successive stages of Drosophila haltere morphogenesis. *Proc. Natl. Acad. Sci. USA* **108**, 2855-2860. doi:10.1073/pnas.1015077108

Petryk, A., Warren, J. T., Marqués, G., Jarcho, M. P., Gilbert, L. I., Kahler, J., Parvy, J.-P., Li, Y., Dauphin-Villemant, C. and O'Connor, M. B. (2003). Shade is the Drosophila P450 enzyme that mediates the hydroxylation of ecdysone to the steroid insect molting hormone 20-hydroxyecdysone. *Proc. Natl. Acad. Sci. USA* **100**, 13773-13778. doi:10.1073/pnas.2336088100

Rewitz, K. F., Rybczynski, R., Warren, J. T. and Gilbert, L. I. (2006). Developmental expression of Manduca shade, the P450 mediating the final step in molting hormone synthesis. *Mol. Cell. Endocrinol.* **247**, 166-174. doi:10.1016/j.mce.2005.12.053

Riddiford, L. M., Cherbas, P. and Truman, J. W. (2000). Ecdysone receptors and their biological actions. *Vitam. Horm.* **60**, 1-73. doi:10.1016/S0083-6729(00)60016-X

Roch, F. and Akam, M. (2000). Ultrabithorax and the control of cell morphology in Drosophila halteres. *Development* **127**, 97-107. doi:10.1242/dev.127.1.97

Schubiger, M. and Truman, J. W. (2000). The RXR ortholog USP suppresses early metamorphic processes in Drosophila in the absence of ecdysteroids. *Development* **127**, 1151-1159. doi:10.1242/dev.127.6.1151

Shahin, R., Iwanaga, M. and Kawasaki, H. (2018). Expression profiles of cuticular protein genes in wing tissues during pupal to adult stages and the deduced adult cuticular structure of Bombyx mori. *Gene* **646**, 181-194. doi:10.1016/j.gene.2017.11.076

Struhl, G. (1982). Genes controlling segmental specification in the Drosophila thorax. *Proc. Natl. Acad. Sci. USA* **79**, 7380-7384. doi:10.1073/pnas.79.23.7380

Tomoyasu, Y. (2017). Ultrabithorax and the evolution of insect forewing/hindwing differentiation. *Curr Opin Insect Sci* **19**, 8-15. doi:10.1016/j.cois.2016.10.007

Tomoyasu, Y., Wheeler, S. R. and Denell, R. E. (2005). Ultrabithorax is required for membranous wing identity in the beetle Tribolium castaneum. *Nature* **433**, 643-647. doi:10.1038/nature03272

Wakimoto, B. T. and Kaufman, T. C. (1981). Analysis of larval segmentation in lethal genotypes associated with the antennapedia gene complex in Drosophila melanogaster. *Dev. Biol.* **81**, 51-64. doi:10.1016/0012-1606(81)90347-X

Wang, H.-B., Moriyama, M., Iwanaga, M. and Kawasaki, H. (2010). Ecdysone directly and indirectly regulates a cuticle protein gene, BMWCP10, in the wing disc of Bombyx mori. *Insect Biochem. Mol. Biol.* **40**, 453-459. doi:10.1016/j.ibmb.2010.04.004

Weatherbee, S. D., Halder, G., Kim, J., Hudson, A. and Carroll, S. (1998). Ultrabithorax regulates genes at several levels of the wing-patterning hierarchy to shape the development of the Drosophila haltere. *Genes Dev.* **12**, 1474-1482. doi:10.1101/gad.12.10.1474

Weatherbee, S. D., Nijhout, H. F., Grunert, L. W., Halder, G., Galant, R., Selegue, J. and Carroll, S. (1999). Ultrabithorax function in butterfly wings and the evolution of insect wing patterns. *Curr. Biol.* **9**, 109-115. doi:10.1016/S0960-9822(99)80064-5

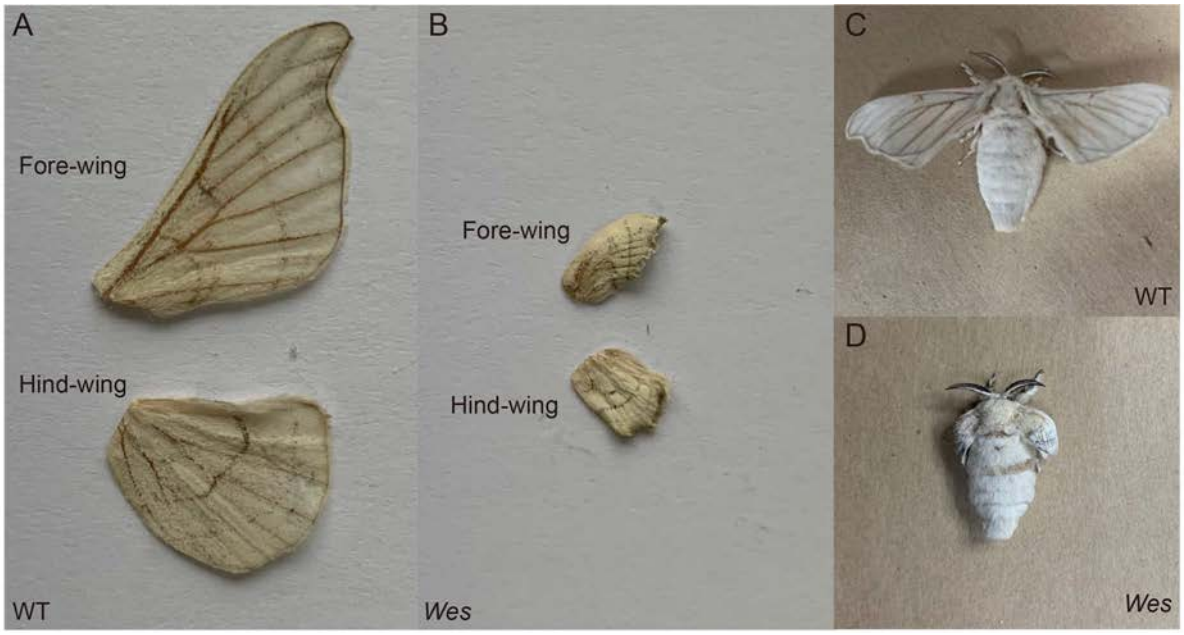

Fig. S1. The phenotypes of Wes (*Antp*$^{+/-}$) mutant. (A, B) The adult forewings and hindwings of WT and *Wes*. (C, D) Morphology of WT and Wes adult males. Their sex are male.

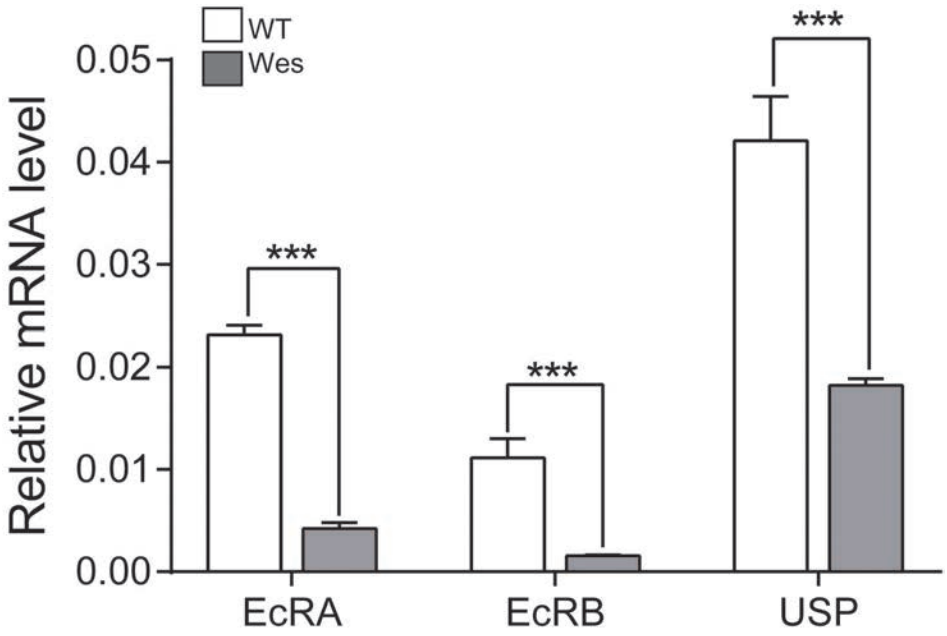

Fig. S2. Changes in the expression levels of 20E nuclear receptors genes in Wes mutant (Antp$^{+/-}$) at the 4th day of the pupal stage. All experimental data shown are means ± SE (n=3). Asterisks indicate significant differences with a two-tailed t-test:

*P < 0.05, **P < 0.01, and ***P < 0.001.

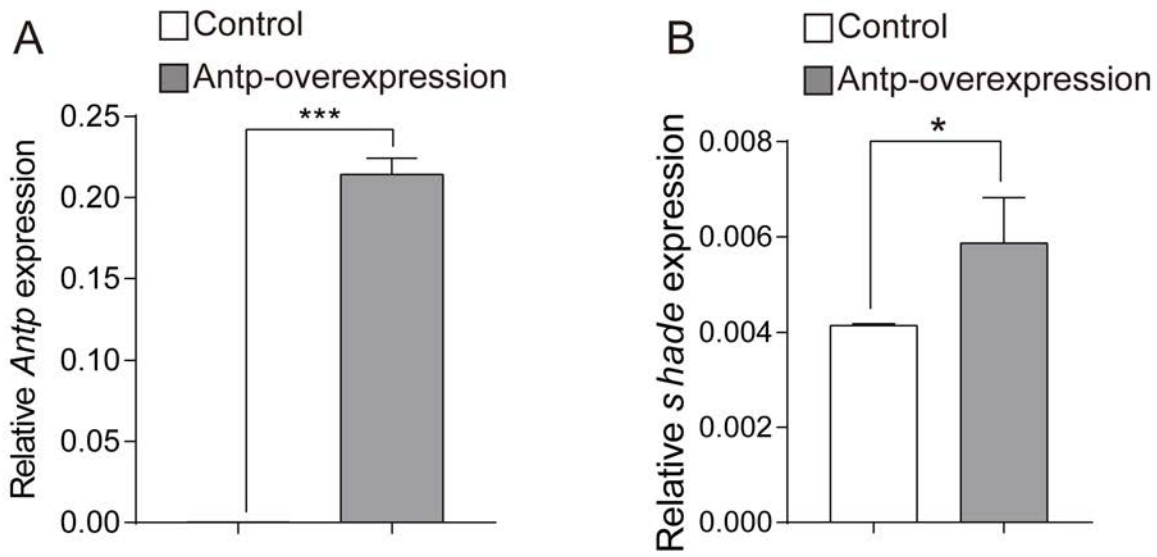

Fig. S3. mRNA levels of *Antp* and s*hade* after transient transfection of Antp overexpression vectors.

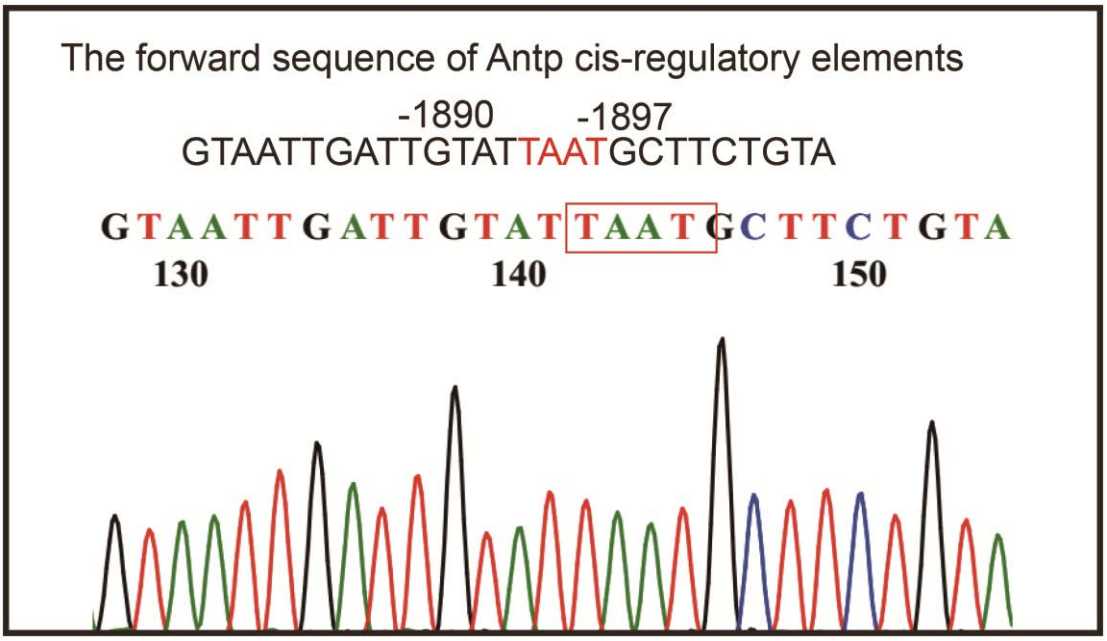

Fig. S4. Sequence of the nt -1897– -1890 region in the shade promoter.

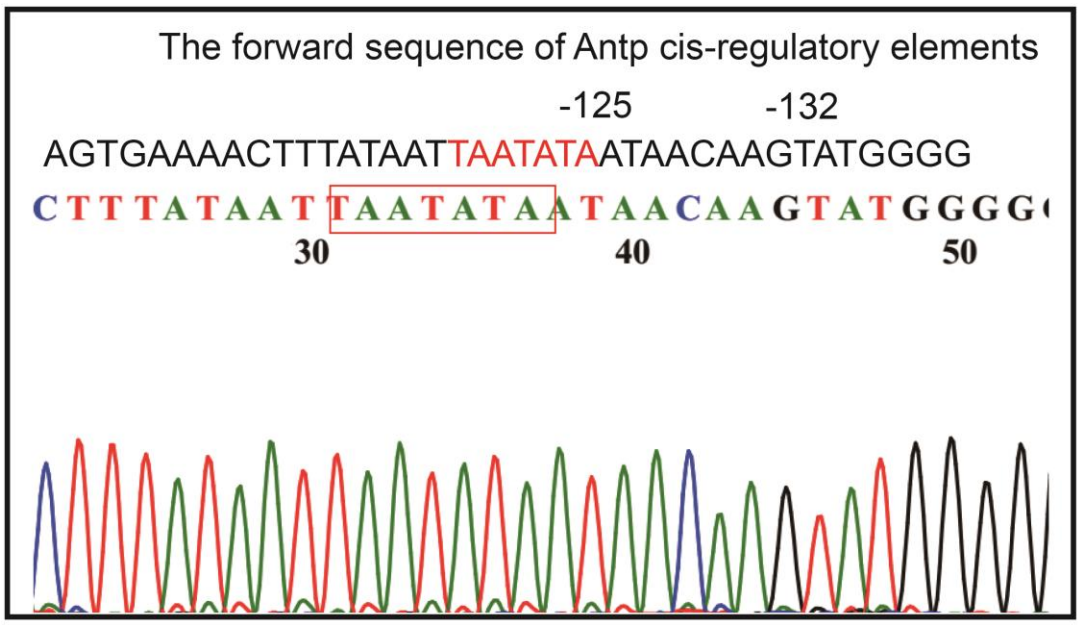

Fig. S5. Sequence of the nt -125– -132 region in the *CPH28* promoter.

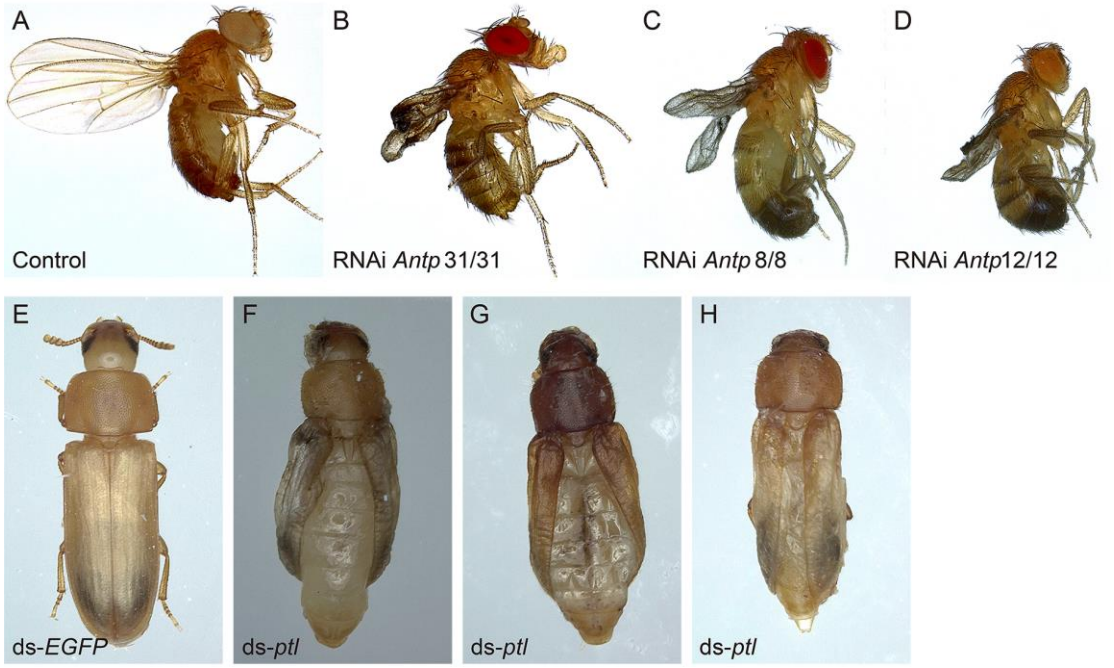

Fig. S6. Knockdown of *Antp* disrupts normal wing development in *Drosophila* and *Tribolium*. (A-D) In *Drosophila*, adult wings of the control flies *yw* appeared as normal phenotypes. *Antp* knockdown flies *nub-gal4>UAS-Antp*^{RNAi} had holdout phenotypes of rudimentary adult wings. Eight *UAS-Antp*^{RNAi} males and 8 *nub-gal4* virgin females per group and finally generated 31, 8, and 12 *Antp* RNAi offspring at adult stage in three biological replicates, respectively. (E-H) Phenotypes of dsRNA-treated *Tribolium*. ds-*EGFP* treatment individuals were used as control. Two *Antp* RNAi experiments were performed. A total of 85% (218 out of 257) *ptl* (*Antp*) dsRNA treated individuals got the deficient wing morphology, but the analogous wing defect in the control injected with the dsRNA of *EGFP* had not been observed.

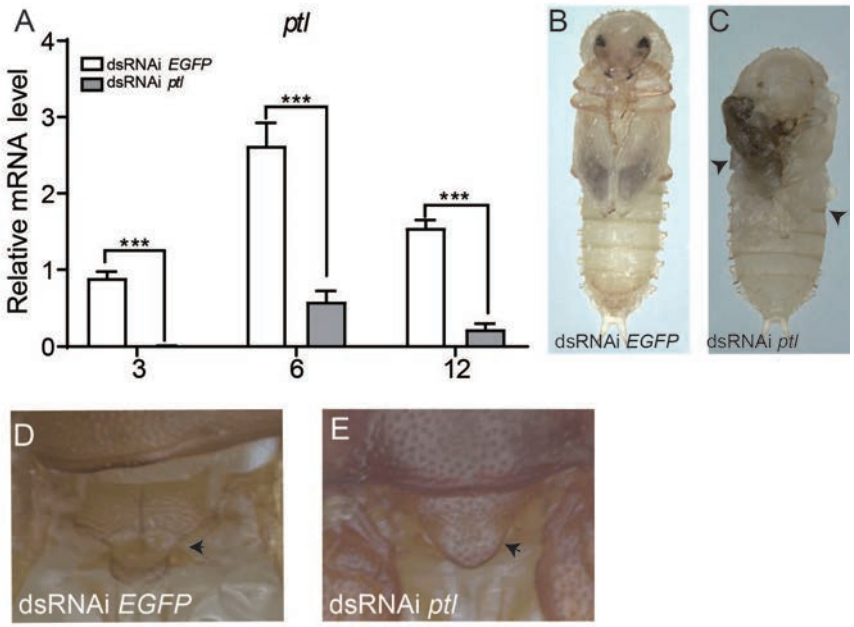

Fig. S7. Loss of *ptl* in *Tribolium* disrupts wing and mesonotum development. (A) The expression levels of *ptl* in *Tribolium*, which were treated with ds*ptl* after 3, 6, and 12 days, respectively, were significantly downregulated. (B and C) The phenotype of the pupa in *ptl* RNAi. B ds-EGFP. C ds-ptl. Black arrows indicate the position of abnormal pupal wing discs. (D and E) The different phenotype of mesonotumin control and *ptl* RNAi (black arrow in D and E). All of the experimental data shown are means ± SE (n=3). Asterisks indicate significant differences with a two-tailed t-test: ***$P < 0.001$.

Table S1. The primers used in this study

Primer name	Forward sequence (5′-3′)	Reversed sequence (5′-3′)	Purpose
Antp	AGACGCAGATGCCCCCTATG	ACCGGGTGTAGGTTTGTCGA	qRT-PCR
Shade	AAGGCTGCCATTATCGACTT	AAGCATTGCATACGGTGGTA	qRT-PCR
Spookier	GGACATCCGATCCTTCATCT	TCTTCGTGTAGCACCCTGAG	qRT-PCR
Shroud	TGTGATAGTGGACTCGGTTGGGC	GGCTTTCGCTGCTTCGGTTTC	qRT-PCR
Shadow	TCGAGGAAGGGACTCCAGTAATAGC	CAAATGGCAGTGTGGCAGATGGTAC	qRT-PCR
Disembobied	TGGGTAGTGAACATGCCAGT	ATCTAAAGCTTCGGCGTCAT	qRT-PCR
EcR A	GCTTCAAGCATAAATGGC	TCAGTCGTTGTAGTGGTAT	qRT-PCR
EcR B	AGCAGCCGTCGCTGGTAGAA	TCGGTCAGCACGCTCAGGAT	qRT-PCR
USP	TTGCTGGCATTGTTTACG	ATCGCACATCATCGCTAC	qRT-PCR
CPH28	GCAGCAGGTGGAAGACTCTT	TCGTATTGGTCAGCCGGAAC	qRT-PCR
CPG9	CCCTCTCAACGAGTACGGTAC	AGTCACTGCGGCAATGAGT	qRT-PCR
CPG11	ATTAATGAGATCGTCCTTACTCCTG	CTCGCTTGTCTTGTTTCTTAGGTTC	qRT-PCR
CPG24	CAATGAAGTACACGGTTATTTTGG	GTCATAGATGCCCCTTTTGTC	qRT-PCR
CPR34	GTCAAACCTCACATTCGCAACC	GGAGTTGGTCTTCCACTTGCTG	qRT-PCR
CPR78	AACGTTGGCAATACTGGGGT	GTATGGGTCTGAGCGCCTC	qRT-PCR
Sw22934	TTCGTACTGCTCTTCTCGT	CAAAGTTGATAGCAATTCCCT	qRT-PCR
ptl	CCTGTACCCCTGGATGAGGA	CGCCTTTGGTCTTGTTCTCC	qRT-PCR
TcCPH28	ACCTGTGACAGTTGCACCAA	GTAGGACGATGGTGTGGTGG	qRT-PCR
TcCyp314a1	TGGGCTTGGTACTACCTGGA	ACTTGCCACCCGCTTTAAGA	qRT-PCR
rsp3	TCAAATTGATCGGAGGTTTG	GTCCCACGGCAACATAATCT	qRT-PCR
Site 1	TAATACGACTCACTATAGGGATGGCTGCGATCAGCAGCT CGTTTTAGAGCTAGAAATAGC	AAAAGCACCGACTCGGTGCCACTTTTT CAAGTTGATAACGGACTAGCCTTATTTT AACTTGCTATTTCTAGCTCTA AAAAGCACCGACTCGGTGCCACTTTTT CAAGTTGATAACGGACTAGCCTTATTTT AACTTGCTATTTCTAGCTCTA	sgRNA construction
Site 2	TAATACGACTCACTATAGGGCTGCGATCAGCAGCTCAGG CGTTTTAGAGCTAGAAATAGC		sgRNA construction
Site 3	TAATACGACTCACTATAGGGGCCGGCACAGCATCACTAC CGTTTTAGAGCTAGAAATAGC		
Site 4	TAATACGACTCACTATAGGGCGCCTGGAATGCCCTACCC CGTTTTAGAGCTAGAAATAGC		
Antp-check	GTCACGAACATCAACAGGCG	ACCATATGCTGTTGGGGGTG	Mutation detection
Shade-2512	CAATTTCGCCGTTTACCGCT	GATAATCAGTTTGAGTTCACAA	Truncated promoter
Shade -2000	ATCACCTTCAACATAGGTCT		
Shade -1500	ACACCTGAGATAATCGTTCCG		
Shade -874	TGCTCGGCTTGCTATCTTGCT		
Shade -600	GGAATGTTATCAGCATTGAAG		
Shade -300	CAACGCGCCCGCGGACGATAT		
CPH28-2194	AATTACCTACTGACGTGTAT	TTGTTGTTTTTTTTTCACTTGTCACTC GC	
CPH28-1711	TAAAAATATCCAAAATAACCA		
CPH28-376	GCAGTTCACAAAAATTTACTT		
dsRNA synthesis *GFP*	TAATACGACTCACTATAGGGACGTAAACGGCCACAAGTT C	TAATACGACTCACTATAGGGTGCTCAGG TAGTGGTTGTCG	dsRNA synthesis
dsRNA synthesis *Antp*	TAATACGACTCACTATAGGGGCGGGGTCGACAAACCTAC A	TAATACGACTCACTATAGGGGTAACTTC GGCCTTCGGACC	
dsRNA synthesis *ptl* 1	TAATACGACTCACTATAGGGATGAGTTCATATTTCGCCA A	TAATACGACTCACTATAGGGCCCATGTG ATGGTTGTTCAT	
dsRNA synthesis *ptl* 2	TAATACGACTCACTATAGGGCACCAAACGCAGGTGGTCT A	TAATACGACTCACTATAGGGCGCCTTTG GTCTTGTTCTCC	dsRNA synthesis
CPH28 RNAi 1	GCAGCAAUUGUUCGCACAATT	UUGUGCGAACAAUUGCUGCTT	RNA interference
CPH28 RNAi 2	GGAAGCUUUACAUUCGGUUTT	AACCGAAUGUAAAGCUUCCTT	
Shade probe	CAGTAATTGATTGTATTAATGCTTCTGT	ACAGAAGCATTAATACAATCAATTACT G	Probe
CPH28 probe	AACTTTATAATTAATATAATAACAAGTATG	CATACTTGTTATTATATTAATTATAAA GTT	
Shade mutation probe	CAGTAATTGATTAAAAGGGGGCTTCTGT	ACAGAAGCCCCCTTTTAATCAATTACT G	Mutated probe
CPH28 mutation probe	AACTTTATAATAAAAGGGGACAAGTATG	CATACTTGTCCCCTTTTATTATAAAGTT	
Shade- ChIP	ACCTGTTGCAGAGGTAGAACG	TTGCGGCGCAGATAGTGAT	ChIP-PCR
CPH28- ChIP	AGATCAATTCACGCTCAAAACCC	GCGGGGCACACACTACTAT	

Table S2. Statistical analysis of *BmAntp* gene RNAi experiment

Injection samples	dsRNA concentration (ng/ul)	Injection strain	Normal	Mutant	No. of pupate injected
ds EGFP	17000	*Dazao*	10	0	10
ds Antp	17000	*Dazao*	3	19	22

Table S3. Phenotypic analysis of *CPH28* gene RNAi experiment

Injection samples	siRNA concentrantion (ug/ul)	Injection strain	Normal	Partially mutant	Mutant	No. of pupa injected
Negative si RNA	1	*Dazao*	12	0	0	12
CPH28 si RNA	1	*Dazao*	3	3	6	12